Research Papers

The role of polymer gel electrolyte infiltration for enhancement of capacitance and cycle stability

Bilge Saruhan [*], Apurba Ray

Institute of Materials Research, German Aerospace Center (DLR), 51147 Cologne, Germany

ABSTRACT

With the increasing application of electronic materials in various fields such as flexible electronic textiles, wearable and portable gadgets, aerospace and aircraft systems etc., the demand for clean high-power energy storage devices is also increasing rapidly. To date, the application of market available supercapacitors has not met the energy expectations in the range of market leading Li-ion batteries (LIBs) due to their unreliable mechanical flexibility, electrolyte leakage, low voltage application, low capacity, low cycle stability and moderate rate-capability. Inappropriate utilization of the maximum porosity of the electrode material and inefficient activities of the electrode/electrolyte interface are major challenges for present supercapacitor development. In this work, for the first time, the role of polymer gel electrolyte infiltration to improve the electrochemical performance of a supercapacitor has been explicitly studied and investigated. It has been observed that 1-Ethyl-3-Methylimidazolium bis(trifluoromethylsulfonyl)imide [EMIM][TFSI] ionic liquid electrolyte embedded in Polypropylene Carbonate (PPC) and Polycarbonate (PC) polymer matrix polymer gel electrolyte (PGE) showed excellent supercapacitive performance at high voltage window 2.6 V by delivering maximum total capacitance of 5.81 F and maximum energy density 10.9 Wh kg^{-1} at 30 mA current (0.06 A g^{-1}). Regular infiltration of the polymer gel electrolyte inside the electrode material is also observed during long cycle operation of 10,000 cycles. Infiltration of electrolyte ions into the pores of electrode materials plays a significant role in increasing capacitance and cycle Stability. These results highlight the potential of this novel high-voltage polymer gel electrolyte for future high-power energy storage device applications.

1. Introduction

Rapidly increasing demand for energy, depletion of fossil fuels, energy crisis, development of smart portable electronic and high-performance advanced vehicles has attracted a huge attention to search for highly efficient, low cost, stable, and environmentally friendly energy storage systems [1–3]. Nowadays, devices such as smartphones, light-emitting diode (LED) indicators, various smart sensors and Internet of Things (IoTs) systems play a significant role in human lives for 24-hour monitoring of health [4]. An uninterrupted power supply is very important for operating such electronic devices. Among various energy storage systems, electrochemical energy storage devices such as batteries and supercapacitors are known as emerging technologies. Typical batteries such as lithium ion batteries (LIBs), sodium-ion batteries, etc. can provide high energy density by holding a large amount of charge inside the electrodes and large voltage window [5–7]. However, poor power density (< 300 W/kg), high chemical reactivity, higher

charging time (~ 1 h), lower life cycles (< 1500 cycles), high cost and safety concerns motivate to find an alternative for high performance energy storage devices. In this scenario, electrochemical capacitors, more commonly known as supercapacitors, are promising to provide higher capacitance (~ Farad), fast charge/discharge ability, high power density (~10 kW kg^{-1}) and long cycle life (~ 100,000 cycles). According to the charge storage mechanism, supercapacitors can be classified in two categories. In electric double-layer capacitors (EDLCs), electric charges are stored inside the pores of the electrode surface at the electrode/electrolyte interface by non-faradic electrostatic process [8]. Typically, high surface porous carbon-based materials such as activated carbon, graphene, carbon aerogel and carbon nanotube (CNT) work as EDLC's electrode materials. Conversely, in pseudocapacitors charges are stored in the electrode materials by Faradaic redox reactions and/or intercalation of ions into the electrode materials. Numerous types of transition metal oxides (TMOs) such as RuO_2, MnO_2, Fe_2O_3 and V_2O_5 and various conducting polymer such as polyaniline (PANI),

* Corresponding author.
E-mail address: bilge.saruhan@dlr.de (B. Saruhan).

polypyrrole, PEDOT-PSS and polythiophene are promising electrode materials and can be used as pseudocapacitor [9,10]. Although TMOs have been extensively investigated and they exhibited promising supercapacitor performance on a laboratory scale, relatively low electrical conductivity and self-discharge rate hinder their practical applications as supercapacitors. On the other hand, relatively lower energy density of supercapacitors (< 10 Wh kg^{-1}) still limit their widespread applications. The specific capacitance and voltage window of a supercapacitor play a significant role in the energy density of the supercapacitor. According to the energy density formula ($E_m = \frac{1}{2}\, C_{sp}V^2$), there are three possibilities for increasing energy density of a supercapacitor. Increasing the specific capacitance (C_{sp}), increasing the voltage window (V), or increasing both can enhance the energy density of a supercapacitor. Internal microstructures of electrode materials such as nanowires, nanospheres, nanotubes and nanosheets having larger specific surface area are directly related to materials chemical properties and electrochemical reaction rate, which expressively enhance the charge storage efficiency and specific capacitance [11].

The electrolyte is known as one of the vital components for supercapacitor (SC) devices and controls the movement of oppositely charged ions through a suitable solvent and causes ionic conductivity [12]. Electrolytes strongly influence the SC's performance and electrochemical stability [13]. Increasing the cell voltage by enlarging the potential window of an electrolyte has been shown to be a promising approach for enhancing energy density of a SC. There are various types of electrolytes such as liquid electrolytes, quasi-solid (gel electrolytes) and solid electrolytes which have been using for supercapacitor research in the last decades [14,15]. Liquid electrolytes are very useful for batteries and supercapacitors research because of their easy transport of ions between the two electrodes and their life cycle. However, leakage of electrolytes, evaporation of electrolytes in long -cycles operation and/or upon disclosure to ultraviolet radiations etc. make many problems for liquid electrolytes. To overcome these problems, quasi-solid and solid electrolytes have attracted attention in electrochemical energy storage research [16,17].

Although, solid electrolytes usually showed relatively lower ionic conductivity compared to that of liquid electrolytes, polymer electrolytes (PEs), consisting of polymer matrix-based solid and semi-solids, can minimize the aforementioned problems. The conductivity of polymer electrolytes can be improved by introducing various types of ionic inorganic salts, ionic liquids (IL) and nanofillers [18,19]. In this work, the infiltration of ionic liquid embedded in polymer matrix-based electrolytes and its effects on the supercapacitor performance and cycle stability have been extensively studied and reported. Detailed electrochemical analysis by means of cyclic voltammetry (CV), galvanostatic charge discharge (GCD), electrochemical impedance spectroscopy (EIS) and cyclic charge discharge (CCD) of a supercapacitor device has been conducted and intensively investigated for the first time to measure the effects of infiltration on the cyclic stability of a supercapacitor.

2. Experimental section

2.1. Materials

Activated carbon (AC) coated on both sides of aluminum (Al) foil current collectors (thickness 20 μm) (Skeleton$^+$, Tallin, Estonia) has been used as supercapacitor electrodes (thickness 150 μm, mass loading 10 mg cm^{-2}) [20]. 1-Ethyl-3-methylimidazolium bis(trifluoromethylsulfonyl)imide [EMIM][TFSI] (IoLiTec Liquid Technologies GmbH, Heilbronn, Germany), polypropylene carbonate (PPC) (Sigma Aldrich, Taufkirchen, Germany, 94.5 %, Mn=50,000 g mol^{-1},), Propylene carbonates (PC) (MP Biomedicals, LLC, Mn=102.09 g mol^{-1}), acetonitrile (ACN) (Sigma Aldrich, 99 %,), polymer separator (Celgard 3501–4000M-AS40 of pore diameter 64 nm, Gelgard LLC, Charlotte, NC, USA) etc. have been used for this work. All chemicals used in this work are analytical grade and have been used without any additional treatment.

2.2. Synthesis of polymer gel electrolyte (PGE)

5.0 g of polypropylene carbonate (PPC) was first dissolved in 25 mL of acetonitrile (ACN) under vigorous magnetic stirring of 800 rpm at 90 °C for 30 min. After complete dissolution of the PPC, an equivalent amount of [EMIM][TFSI] ionic liquid electrolyte was mixed with the polymer matrix. 3.0 g of propylene carbonates (PC) were also added into the solution as a plasticizer. To make a homogeneous polymer gel electrolyte, the solution was stirred for around 40 min maintaining the same temperature of 90 °C. Subsequently, the solution was cooled down to room temperature for 2 h with continuous stirring and finally a viscous [EMIM][TFSI]/PPC/PC polymer gel electrolyte is obtained. The synthesis of this electrolyte is scalable and can be upscaled without compromising performance by maintaining the same ratio of PPC, PC polymer and [EMIM][TFSI] ionic liquid.

2.3. Fabrication of supercapacitor pouch cell

To fabricate a pouch cell solid-state symmetric supercapacitor (SSC) device, two pieces of activated carbon (AC) coated electrodes of size 5 cm × 5 cm cut from an A4 size skeleton electrode and used as two electrodes. The total active electrode materials mass loading of two electrodes is 500 mg. First, two electrodes have been heated at 100 °C for 30 min in a hot plate to remove the moisture from the surface of the electrodes. A thin layer of as developed [EMIM][TFSI]/PPC/PC polymer gel electrolyte (PGE) is coated on the top surface of two electrodes and kept in a vacuum desiccator overnight. Then, two PGE-coated electrodes have been sandwiched by placing a non-conductive polymer separator [6] to prevent electrical charge between the electrodes (Fig. 1). This fabricated SSC is then encapsulated inside a vacuum chamber to be used for further electrochemical characterizations.

2.4. Electrochemical characterizations

The electrochemical energy storage performance of a fabricated [EMIM][TFSI]/PPC/PC polymer gel electrolyte (PGE) based solid-state symmetric supercapacitor (SSC) has been studied using a GAMRY Reference 3000 (C3 Prozess-und Analysentechnik, GmbH, Haar near Munich, Germany) multi-channel high-performance potentiostat at room temperature by measuring Cyclic Voltammetry (CV), Galvanostatic charge–discharge (GCD), Electrochemical Impedance Spectroscopy (EIS) and cyclic charge discharge (CCD). Various electrochemical energy storage parameters such as total capacitance (C_T; F), specific capacitance (C_{sp}; Fg^{-1}), energy density (E_m; W h kg^{-1}) and power density
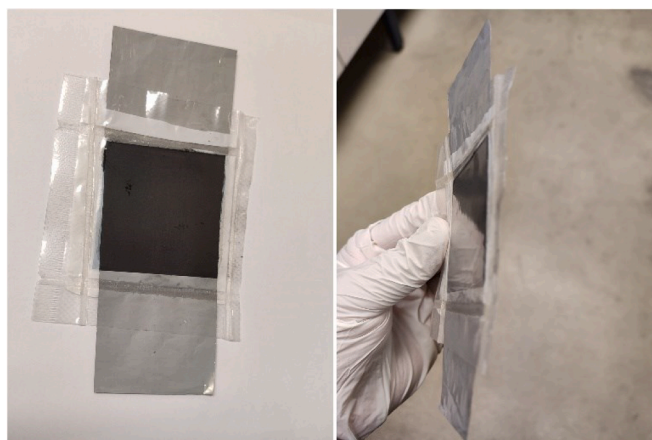

Fig. 1. [EMIM][TFSI]/PPC/PC polymer gel electrolyte-based pouch cell supercapacitor (5 cm × 5 cm).

$(P_m; W kg^{-1})$, respectively of the pouch cell supercapacitor have been calculated using Eqs. (1)–(4);

$$C_T = \frac{I \times \Delta t}{\Delta V} \tag{1}$$

$$C_{sp} = \frac{C_T}{m} \tag{2}$$

$$E_m = \frac{1}{2 \times 3.6} \times C_{sp} \times \Delta V^2 \tag{3}$$

$$P_m = \frac{3600 \times E_m}{\Delta t} \tag{4}$$

where I is the charge-discharge current (A), Δt is the discharge time (s), ΔV is the voltage window and m is the total active electrode mass of two electrodes [2,21].

3. Results and discussions

To get information about the maximum electrochemically-stable operational voltage window of a supercapacitor, the cyclic voltammetry (CV) measurement at a fixed scan rate of 80 mVs^{-1} has been carried out at various voltage windows (0–1.8 V, 0–2.0 V, 0–2.2 V, 0–2.4 V, 0–2.6 V and 0–2.8 V). The nature of all CV curves (Fig. 2a) is similar and quasi-rectangular indicating that this PGE based pouch cell supercapacitor can be expected to operate safely in 0 to 2.8 V voltage window without significant degradation. The quasi-rectangular nature of CV curves with absence of any redox peaks also specifies the non-faradic electric double layer (EDL) charge storage properties of this SC device with a developed [EMIM][TFSI]/PPC/PC polymer gel electrolyte (PGE). There is no sharp increase of current due to unwanted gas evolution such as O_2 or H_2 observed at the edges of the higher working voltage, which also implies the electrochemical stability of the [EMIM][TFSI]/PPC/PC electrolyte as well as SC device [22,23]. In this work, 0 to 2.6 V voltage window for this SSC has been chosen for further electrochemical studies and details analysis. The CV curves (Fig. 2b) measured at different applied scan rates from 5 mVs^{-1} to 100 mVs^{-1} showing a similar quasi-rectangular nature without any distortion. Absence of any redox peaks and presence of quasi-rectangular nature in every CV curve from lower scan rate to higher scan rate clearly indicates EDLC charge storage mechanism and fast charge-discharge capability for this SC. In general, the total amount of charge stored in the device or specific capacitance of the SC device can be calculated from the area covered inside the CV curve at a fixed scan rate using Eq. (5) as follow.

$$C_{sp} (Fg-1) = \frac{\int_{V_a}^{V_c} i\,(V)\,dV}{2 \times m \times \vartheta \times (V_c - V_a)} \tag{5}$$

where υ represents scan rate (V s^{-1}) and $(V_c - V_a) = \Delta V$ is the voltage window [24].

Fig. 2b shows that the CV current increased with increase of scan rate from 5 mVs^{-1} to 100 mV s^{-1}. The increase of CV current with an increasing scan rate and fixed voltage can be described by the movement of electrolyte ions towards oppositely charged electrodes. In general, at a lower scan rate, two ion EMIM$^+$ and TFSI$^-$ get a sufficient amount of time to access the entire outer and inner surface (including the pores) of the electrode materials. Because of this, a large amount of charge can infiltrate the pores and occupy a maximum number of pores, which leads to high capacitance values at lower scan rates [25]. However, as the scan rate increases to the upper-end of the range, the charge mobility per unit time increases. This means that the number of positive and negative ions from the electrolytes move very fast toward the electrode surface but are not given enough time to occupy the pores. Therefore, charges can only accumulate on the surface of the electrode materials at the electrode/electrolyte interface and capacitance value becomes lower [26].

The galvanostatic charge-discharge (GCD) curves (Fig. 3a) measured at various applied currents (30 mA, 50 mA, 70 mA, 100 mA, 130 mA and 150 mA) in a fixed voltage window (0 to 2.6 V) similar to CV (Fig. 2b) shows typical non-faradic EDLC behavior of charge storage process for this [EMIM][TFSI]/PPC/PC electrolyte-based SSC. The symmetric charge-discharge nature or almost ideal triangular shape of the GCD curves implies promising capacitive properties and good capacitive retention [27]. A very small IR drop observed at the beginning of the discharge curve (Fig. 3a) reveals very low electrochemical series resistance or contact resistance (R$_s$) due to the contribution of conductive polymer gel electrolyte. The GCD curves in Fig. 3a also shows that the discharge time decreases with increasing current from 30 mA to 150 mA, which can be explained similarly to charge mobility per unit time like CV current in Fig. 2b. As capacitance value of a device is proportional to the discharge time, the total capacitance and various energy storage parameters such as specific capacitance (F g^{-1}), energy density (W h kg^{-1}) and power density (W kg^{-1}), respectively have been calculated from GCD curves (Fig. 3a) using Eqs. (1)–(4) and represented in Table 1. It has been observed that this SSC offered maximum total capacitance of 5.81 F at 30 mA (0.06 A g^{-1}) and capacitance value decreased with increase of discharge current (Fig. 3b). The decrease in capacitance with increasing discharge current is mostly due to the decrease in the ability of the electrolyte ions to infiltrate the pores of the electrode. This SSC also delivered maximum energy density of 10.9 Wh kg^{-1} at 30 mA (0.06 A g^{-1}) which is based on our knowledge relatively higher compared to current market available supercapacitor devices. The Ragone plot (Fig. 3c) also
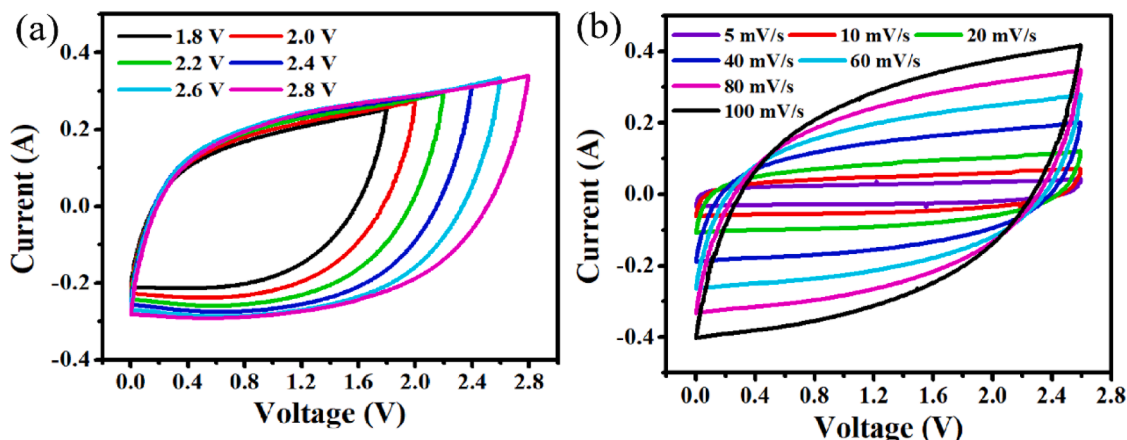

Fig. 2. Cycle voltammetry (CV) curves at (a) different voltage windows and (b) different scan rate of this pouch cell supercapacitor.
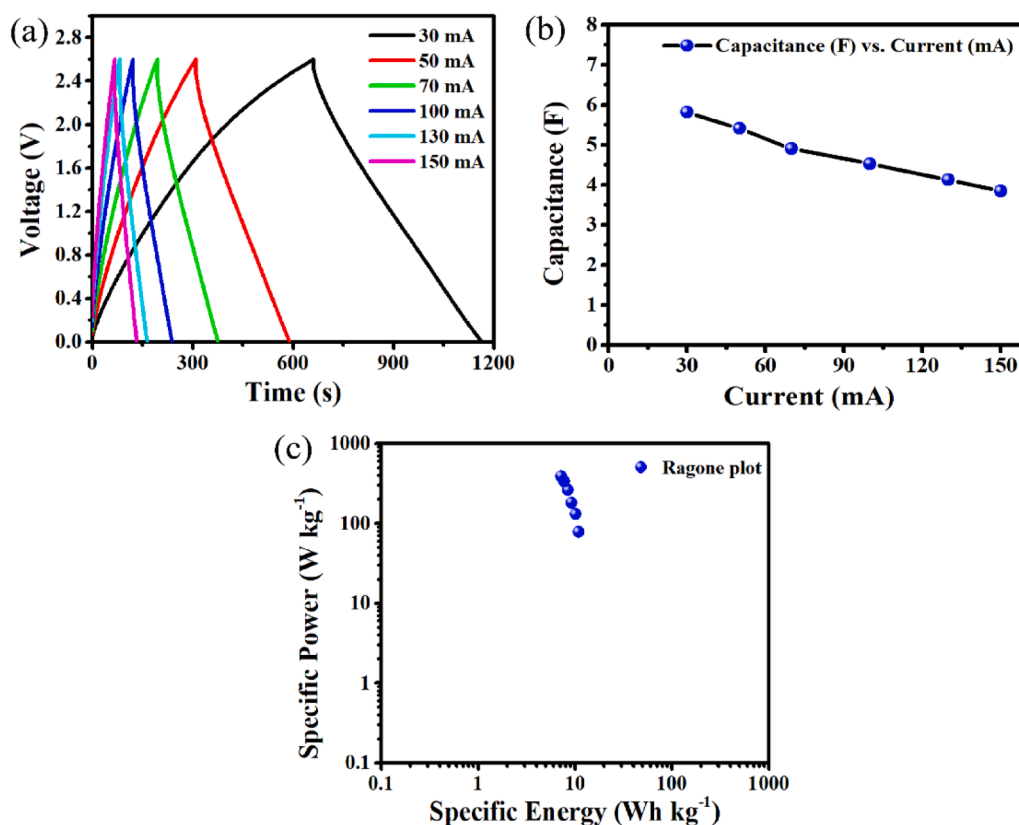
Fig. 3. (a) GCD curves at different current, (b) capacitance (F) vs current (mA) plots and (c) Ragone plot for this pouch cell supercapacitor.

Table 1
Values of various charge storage parameters calculated from GCD curves in Fig. 3a.

Current (mA)	Current density (A g^{-1})	Total Capacitance (F)	Specific capacitance (F g^{-1})	Energy density (Wh kg^{-1})	Power density (W kg^{-1})
30	0.06	5.81	11.6	10.9	78
50	0.10	5.40	10.8	10.1	130
70	0.14	4.90	9.8	9.2	182
100	0.20	4.52	9.1	8.5	260
130	0.26	4.12	8.2	7.7	338
150	0.30	3.84	7.6	7.2	390

shows the variation of specific power density and specific energy density for these pouch cell supercapacitors. It reveals that the SC delivers its maximum specific energy density (10.9 Wh kg^{-1}) at its lowest power density (78 W kg^{-1}). The opposite effect is also shown because the lowest energy density (7.2 Wh kg^{-1}) occurs at the highest power density (390 W kg^{-1}).

To investigate the life cycles and stability of the [EMIM][TFSI]/PPC/PC electrolyte-based pouch cell symmetric supercapacitor, the cyclic charge-discharge (CCD) has been tested for 10,000 cycles at a constant current of 30 mA (0.06 A g^{-1}) at the fixed voltage of 2.6 V. Some interesting charge- discharge behaviors have been observed during this CCD measurement, and this SSC takes almost 30 days to finish 10,000 cycles. It has been observed that the total charge-discharge time (CDT) starts to gradually increase up to 160th cycles and the capacitance value also increased almost 6 times that of first cycle (Fig. 4). Then, CDT gradually decreases with an increase in the number of cycles, but an increase and decrease in total CDT can be observed regularly with an increase in the number of cycles. The initial increase in charge discharge time and capacitance value is due to the normal electrochemical activation of the electrode materials as well as the electrolyte ions from
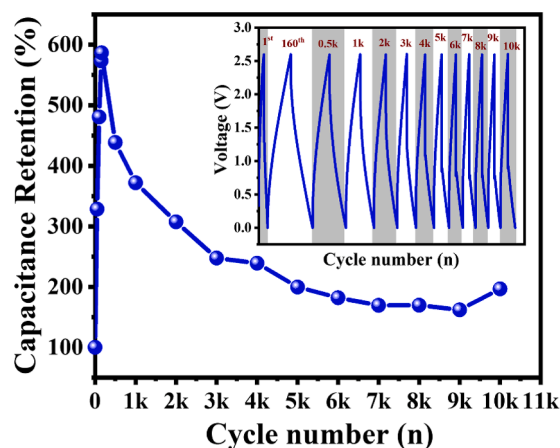

Fig. 4. Capacitance retention vs cycle number and CCD plots (inset) of this pouch cell supercapacitor.

polymer gel electrolyte occupying free space inside the pores [28,29]. The synergistic effect between IL and polymer matrix also plays a significant role in the initial increase of the capacitance values of the supercapacitors [18,30,31]. For this SSC, the maximum discharge time was reached at around the 160th cycle. Following this peak, the discharge time decreased; this may have been due to a decrease in unoccupied pores on the electrode surface at the interface. Additionally, it is a possibility that repulsive forces from already occupied ions repelled ions from the electrolytes [31–33]. The increase and decrease in CDT as a result of the increase in the number of cycles (3k to 4k, 7k to 8k and 9k to 10k, respectively) (Fig. 4 inset) is mainly due to the continuous infiltration effect of the [EMIM][TFSI]/PPC/PC polymer electrolyte inside the layer of electrode materials. Infiltration of polymer electrolyte

significantly enhance the supercapacitive performance the pouch cell and enhance its lifetime [34,35]. This pouch cell supercapacitor exhibited good electrochemical stability over 10,000 cycles which is explained from EIS studies.

To get detailed information about the charge storage performance of this SC, the electrochemical impedance has been measured at different times during the experiment; the impedance is measured at the beginning of the experiment, after CV measurement and after CCD measurement. A frequency range of 100 kHz to 0.01 Hz, an AC perturbation amplitude of 10 mV and a DC potential of 0 V are used to accomplish this. All EIS curves (Fig. 5a) show two distinct regions such as a depressed semicircle at the high frequency (100 kHz) corresponding to the charge transfer resistance (R_{ct}) and a straight line almost parallel to the Y-axis in the very low frequency region (0.01 Hz) corresponding to the ion diffusion control Warburg impedance (W_0). The intersection of the X-axis provides the information about electrochemical series resistance (R_s), corresponding to the electrolyte resistance and contact resistance at electrode/current collector interface [36]. The EIS nature (Fig. 5a) of this pouch cell shows very low overall cell impedance ($<$ 5 Ω) and contact resistance ($R_s \sim$ 0.3 Ω), which is very important for supercapacitor device fabrication for real application. It has been observed that total impedance is highest at the beginning of experiment (black line) and decreases after CV measurements (red line). The decrease of impedance is mainly due to the infiltration of the polymer gel electrolyte within the electrode materials enhancing the conductivity as well as capacity of the SC device. The electrochemical series resistance (R_s) and charge transfer resistance (R_{ct}) also decreased (Fig. 5b) as the time of device operations (CV, GCD etc.) increased which strongly confirmed that the infiltration of polymer gel electrolyte played a significant role for enhancement of capacitance and cycle stability for a supercapacitor. In this [EMIM][TFSI]/PPC/PC polymer electrolyte the polypropylene carbonate (PPC) polymer matrix provides a cross-linked spatial network structure to offer a secondary skeleton to the Propylene carbonates (PC) plasticizer to be filled in the structural gap. Addition of this PC plasticizer in the PPC polymer matrix also improved the conductivity and flexibility of the [EMIM][TFSI]/PPC/PC polymer gel electrolyte preventing the leakage of the electrolyte during long cycle operation. A small distortion and impedance increase are observed after the CCD test which may be due to poor electrical contact at the electrode/electrolyte interface during CCD measurement due to the formation of some air gaps from low vacuum packaging of the pouch cell, resulting in higher R_s. However, the overall EIS studies show that this [EMIM][TFSI]/PPC/PC polymer gel electrolyte perform very good and it is useful for high-power energy storage device applications.

The phase angle vs. frequency plot, known as Bode plot (Fig. 6a) measured at different operation time for this pouch cell supercapacitor shows that the phase angle approach towards 90° at low frequency of 0.01 Hz for each time such as beginning of experiment, after CV measurement and after CCD measurement. For an ideal capacitor, the phase angle approaches 90° at low frequency, which also confirms that this [EMIM][TFSI]/PPC/PC polymer gel electrolyte-based supercapacitors maintains almost ideal EDLC behavior without any degradation or distortion of the phase angle curves. It has also been observed that maximum capacitance value comes from non-faradic surface-controlled double-layer charge accumulation contribution without any electrochemical degradation of [EMIM][TFSI] ionic liquid embedded polymer gel electrolyte in high voltage operation and enhancing the cycle stability as well.

In order to investigate the possibility of use of this pouch cell supercapacitor stored energy, a hand-on demonstration has been performed using a laboratory made propeller. It has been observed that the propeller run (Fig. 6b) for $>$20 min after charging the pouch cell supercapacitor for 60 second. This demonstration indicates the potential use of these high voltage ($>$2.6 V) [EMIM][TFSI]/PPC/PC polymer gel electrolyte-based supercapacitors in future structure integrated various aerospace applications.

4. Conclusion

In conclusion, a new type of [EMIM][TFSI]/PPC/PC polymer gel electrolyte has been successfully developed using [EMIM][TFSI] ionic liquid as active electrolyte embedded in PPC and PC polymer matrix in a suitable proportion. High voltage supercapacitive performance of this polymer gel electrolyte has been intensively investigated by fabricating a 5 cm × 5 cm pouch cell with activated carbon-based standard electrode. This symmetric pouch cell supercapacitor offers a maximum capacitance of 5.81 F and energy density of 10.9 Wh kg^{-1} at high voltage window of 2.6 V. Based on the knowledge reported here, the role of polymer gel electrolyte infiltration for the enhancement of capacitance and cycle stability of a supercapacitor. Also confirmed by EIS studies, an increase and decrease in total charge discharge time on a regular basis with increase in cycle number has been observed due to the continuous infiltration effect of [EMIM][TFSI]/PPC/PC polymer gel electrolyte within the electrode materials. This pouch cell shows promising long cycle performance over 10,000 cycles at a high voltage of 2.6 V. The overall electrochemical studies confirm that this new [EMIM][TFSI]/PPC/PC polymer gel electrolyte possesses a potential to be used for peak energy storage for aerospace, aircraft and various domestic applications as well. We expect that the present work will provide readers and researchers with new information and open new doors in polymer electrolyte based electrochemical energy storage research of supercapacitor and batteries.
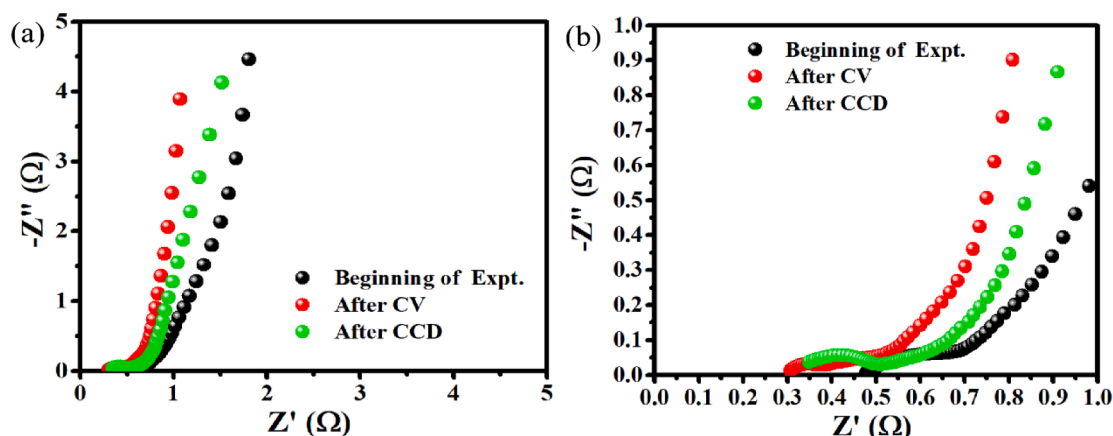

Fig. 5. (a) complete EIS curves and (b) EIS curves at high frequency region of this pouch cell supercapacitor.
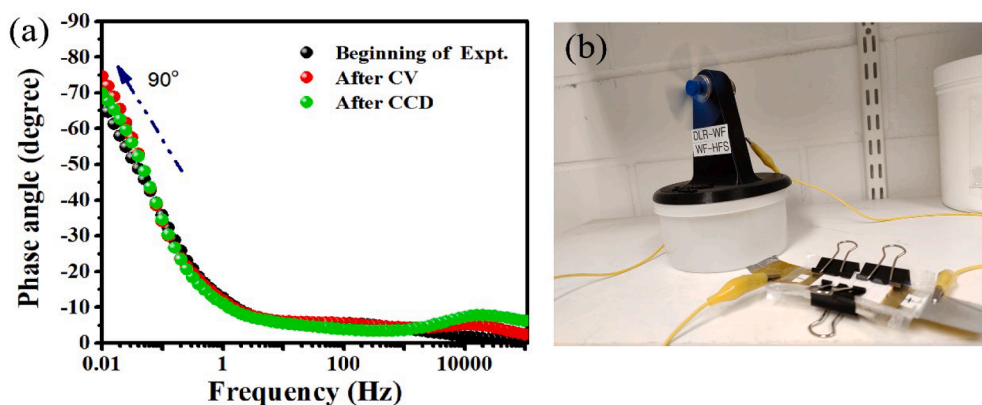
Fig. 6. (a) Bode plot and (b) hand-on demonstration of this pouch cell supercapacitor.

CRediT authorship contribution statement

Bilge Saruhan: Writing – review & editing, Validation, Supervision, Resources, Project administration, Investigation, Formal analysis, Conceptualization. **Apurba Ray:** Writing – review & editing, Writing – original draft, Investigation, Formal analysis, Data curation, Conceptualization.

Declaration of competing interest

The authors declare that they have no known competing financial interests or personal relationships that could have appeared to influence the work reported in this paper.

Data availability

Data will be made available on request.

Acknowledgments

References

[1] R. Muchakayala, S. Song, J. Wang, Y. Fan, M. Bengeppagari, J. Chen, M. Tan, Development and supercapacitor application of ionic liquid-incorporated gel polymer electrolyte films, J. Ind. Eng. Chem. 59 (2018) 79–89, https://doi.org/10.1016/j.jiec.2017.10.009.

[2] Y. Gong, D. Fu, M. Fan, S. Zheng, Y. Xue, Multilayer Core-Sheath Wires with Radially Aligned N-Doped Carbon Nanohole Arrays for Boosting Energy Storage in Zinc-Ion Hybrid Supercapacitors, ACS Appl. Mater. Interfaces 16 (2024) 4793–4802, https://doi.org/10.1021/acsami.3c16481.

[3] M. Liao, C. Wang, Y. Hong, Y. Zhang, X. Cheng, H. Sun, X. Huang, L. Ye, J. Wu, X. Shi, X. Kang, X. Zhou, J. Wang, P. Li, X. Sun, P. Chen, B. Wang, Y. Wang, Y. Xia, Y. Cheng, H. Peng, Industrial scale production of fibre batteries by a solution-extrusion method, Nat. Nanotechnol. 17 (2022) 372–377, https://doi.org/10.1038/s41565-021-01062-4.

[4] M.M. Ovhal, H.B. Lee, V.V. Satale, B. Tyagi, S. Chowdhury, J.W. Kang, One-meter-long, all-3d-printed supercapacitor fibers based on structurally engineered electrode for wearable energy storage, Adv. Energy Mater. 14 (2024) 1–10, https://doi.org/10.1002/aenm.202303053.

[5] V. Kumaravel, J. Bartlett, S.C. Pillai, Solid electrolytes for high-temperature stable batteries and supercapacitors, Adv. Energy Mater. 11 (2021) 2002869, https://doi.org/10.1002/aenm.202002869.

[6] M.T. Tsehaye, G.T. Gebreslassie, N.H. Choi, D. Milian, V. Martin, P. Fischer, J. Tübke, N. El Kissi, M.L. Donten, F. Alloin, C. Iojoiu, Pristine and modified porous membranes for zinc slurry–air flow battery, Molecules 26 (2021) 4062, https://doi.org/10.3390/molecules26134062.

[7] Q. Wang, X. Xu, B. Hong, M. Bai, J. Li, Z. Zhang, Y. Lai, Molecular engineering of a gel polymer electrolyte via in-situ polymerization for high performance lithium metal batteries, Chem. Eng. J. 428 (2022) 131331, https://doi.org/10.1016/j.cej.2021.131331.

[8] X. He, X. Zhang, A comprehensive review of supercapacitors: properties, electrodes, electrolytes and thermal management systems based on phase change materials, J. Energy Storage 56 (2022) 106023, https://doi.org/10.1016/j.est.2022.106023.

[9] J. Wang, Y. Liu, T. Hao, J. Wang, J. Hao, S. Wang, T. Ma, Y. Hao, Preparation of NiMoO$_4$ porous nanosheets by freezing method as adhesive-free electrodes for high-performance flexible supercapacitors, Ionics (Kiel) 30 (2024) 1749–1758, https://doi.org/10.1007/s11581-024-05379-7.

[10] M. Shi, M. Zhao, Q. Zheng, F. Li, L. Jiao, Z. Su, M. Li, X. Song, Constructing Crystalline NiCoP@Amorphous Nickel-Cobalt Boride Core-Shell Nanospheres with Enhanced Rate Capability for Aqueous Supercapacitors and Rechargeable Zn-Based Batteries, Energy and Fuels 38 (2024) 1525–1537, https://doi.org/10.1021/acs.energyfuels.3c04277.

[11] X. Wei, X. Jiang, J. Wei, S. Gao, Functional groups and Pore size distribution do matter to hierarchically porous carbons as high-rate-performance supercapacitors, Chem. Mater. 28 (2016) 445–458, https://doi.org/10.1021/acs.chemmater.5b02336.

[12] C. Lu, H. Jiang, X. Cheng, J. He, Y. Long, Y. Chang, X. Gong, K. Zhang, J. Li, Z. Zhu, J. Wu, J. Wang, Y. Zheng, X. Shi, L. Ye, M. Liao, X. Sun, B. Wang, P. Chen, Y. Wang, H. Peng, High-performance fibre battery with polymer gel electrolyte, Nature 629 (2024) 86–91, https://doi.org/10.1038/s41586-024-07343-x.

[13] T.S. Bhat, P.S. Patil, R.B. Rakhi, Recent trends in electrolytes for supercapacitors, J. Energy Storage 50 (2022) 104222, https://doi.org/10.1016/j.est.2022.104222.

[14] G.K. Silori, S. Thoka, K.C. Ho, Demonstration of a Gel-polymer electrolyte-based electrochromic device outperforming its solution-type counterpart in all merits: architectural benefits of CeO$_2$ Quantum Dot and Nanorods, ACS Appl. Mater. Interfaces 16 (2024) 4958–4974, https://doi.org/10.1021/acsami.3c16506.

[15] D. Ji, J. Kim, Trend of Developing Aqueous Liquid and Gel Electrolytes for Sustainable, Safe, and High-Performance Li-Ion Batteries, Nano-Micro Lett 16 (2024) 1–18, https://doi.org/10.1007/s40820-023-01220-4.

[16] Z. Song, H. Duan, L. Li, D. Zhu, T. Cao, Y. Lv, W. Xiong, Z. Wang, M. Liu, L. Gan, High-energy flexible solid-state supercapacitors based on O, N, S-tridoped carbon electrodes and a 3.5 V gel-type electrolyte, Chem. Eng. J. 372 (2019) 1216–1225, https://doi.org/10.1016/j.cej.2019.05.019.

[17] Y. Zhao, L. Wang, Y. Zhou, Z. Liang, N. Tavajohi, B. Li, T. Li, Solid polymer electrolytes with high conductivity and transference number of li ions for li-based rechargeable batteries, Adv. Sci. 8 (2021) 1–22, https://doi.org/10.1002/advs.202003675.

[18] K. Mishra, N. Devi, S.S. Siwal, Q. Zhang, W.F. Alsanie, F. Scarpa, V.K. Thakur, Ionic liquid-based polymer nanocomposites for sensors, energy, biomedicine, and environmental applications: roadmap to the future, Adv. Sci. 9 (2022) 1–50, https://doi.org/10.1002/advs.202202187.

[19] K. Aruchamy, S. Ramasundaram, S. Divya, M. Chandran, K. Yun, T.H. Oh, Gel polymer electrolytes: advancing solid-state batteries for high-performance applications, Gels 9 (2023) 585, https://doi.org/10.3390/gels9070585.

[20] J. Petersen, A. Kube, S. Geier, P. Wierach, Structure-Integrated Thin-Film Supercapacitor as a Sensor, Sensors 22 (2022) 6932, https://doi.org/10.3390/s22186932.

[21] A. Ray, J. Roth, B. Saruhan, Laser-induced interdigital structured graphene electrodes based flexible micro-supercapacitor for efficient peak energy storage, Molecules 27 (2022) 329, https://doi.org/10.3390/molecules27010329.

[22] H. Dai, G. Zhang, D. Rawach, C. Fu, C. Wang, X. Liu, M. Dubois, C. Lai, S. Sun, Polymer gel electrolytes for flexible supercapacitors: recent progress, challenges, and perspectives, Energy Storage Mater 34 (2021) 320–355, https://doi.org/10.1016/j.ensm.2020.09.018.

[23] J. Zhu, X. Zheng, Y. Lu, H. Tong, M. Qi, Y. Liu, D. Li, D. Jiang, Synergistic Coupling of CoS$_2$/MoS$_2$ with Polypyrrole as a Highly Efficient and Robust Bifunctional Electrocatalyst for Water Splitting, ACS Sustain. Chem. Eng. 12 (2024) 235–247, https://doi.org/10.1021/acssuschemeng.3c05547.

[24] A. Ray, A. Roy, S. Saha, M. Ghosh, S.R. Chowdhury, T. Maiyalagan, S. K. Bhattacharya, S. Das, Electrochemical energy storage properties of ni-mn-oxide electrodes for advance asymmetric supercapacitor application, Langmuir 35 (2019) 8257–8267, https://doi.org/10.1021/acs.langmuir.9b00955.

[25] A. Ray, A. Roy, P. Sadhukhan, S.R. Chowdhury, P. Maji, S.K. Bhattachrya, S. Das, Electrochemical properties of TiO$_2$-V$_2$O$_5$ nanocomposites as a high performance supercapacitors electrode material, Appl. Surf. Sci. 443 (2018) 581–591, https://doi.org/10.1016/j.apsusc.2018.02.277.

[26] Kanika, Y. Gairola, R. Tomar, S. Kumar, S. Konwar, S.V. Savilov, T. Yadav, M.Z. A. Yahya, P.K. Singh, Supercapacitor using polyvinyl alcohol doped ionic liquid 1-butyl-1-methylpyrrolidinium hexafluorophosphate polymer electrolyte system, Energy Storage 6 (2024) e569, https://doi.org/10.1002/est2.569, 1–8.

[27] H. Xiao, Z.S. Wu, L. Chen, F. Zhou, S. Zheng, W. Ren, H.M. Cheng, X. Bao, One-step device fabrication of phosphorene and graphene interdigital micro-supercapacitors with high energy density, ACS Nano 11 (2017) 7284–7292, https://doi.org/10.1021/acsnano.7b03288.

[28] I.F. Erlangga, S.A. Pradanawati, A.D. Pramata, N.L. Hamidah, Corn starch-sodium acetat composite material from industrial waste fly ash for solid electrolyte polymer ionic conductivity in supercapacitor application, Eng. Chem. 5 (2024) 19–25, https://doi.org/10.4028/p-kqn5dt.

[29] A. Roy, A. Ray, S. Saha, M. Ghosh, T. Das, B. Satpati, M. Nandi, S. Das, NiO-CNT composite for high performance supercapacitor electrode and oxygen evolution reaction, Electrochim. Acta 283 (2018) 327–337, https://doi.org/10.1016/j.electacta.2018.06.154.

[30] H. Ahn, D. Kim, M. Lee, K.W. Nam, Challenges and possibilities for aqueous battery systems, Commun. Mater. 4 (2023) 37, https://doi.org/10.1038/s43246-023-00367-2, 1–19.

[31] W. Chae, B. Kim, W.S. Ryoo, T. Earmme, A brief review of gel polymer electrolytes using in situ polymerization for lithium-ion polymer batteries, Polymers (Basel) 15 (2023) 803, https://doi.org/10.3390/polym15040803.

[32] J.N. Murphy, T. Mendes, F.M. Kerton, D.R. MacFarlane, Biorenewable calcite as an inorganic filler in ionic liquid gel polymer electrolytes for supercapacitors, ACS Omega 8 (2023) 21418–21424, https://doi.org/10.1021/acsomega.2c06876.

[33] A. Ray, D. Korkut, B. Saruhan, Efficient flexible all-solid supercapacitors with direct sputter-grown needle-like Mn/MnO$_x$ @graphite-foil electrodes and PPC-embedded ionic electrolytes, Nanomaterials 10 (2020) 1768, https://doi.org/10.3390/nano10091768.

[34] S. Suriyakumar, P. Bhardwaj, A.N. Grace, A.M. Stephan, Role of polymers in enhancing the performance of electrochemical supercapacitors: a review, Batter. Supercaps 4 (2021) 571–584, https://doi.org/10.1002/batt.202000272.

[35] A. Singh, R. Bhardwaj, R.K. Mishra, A.K. Sundramoorthy, V. Gupta, S. Arya, Potential of functional gel polymers as electrolytes for supercapacitors, Ionics (Kiel) 29 (2023) 3831–3851, https://doi.org/10.1007/s11581-023-05112-w.

[36] A. Ray, A. Roy, M. Ghosh, J.A. Ramos-ramón, S. Saha, U. Pal, S.K. Bhattacharya, S. Das, Study on charge storage mechanism in working electrodes fabricated by sol-gel derived spinel NiMn$_2$O$_4$ nanoparticles for supercapacitor application, Appl. Surf. Sci. 463 (2019) 513–525, https://doi.org/10.1016/j.apsusc.2018.08.259.